7B.4

RAPID INTENSIFICATION OF HURRICANE EARL IN ADVANCED HURRICANE WRF MODEL SIMULATIONS

Diamilet Pérez-Betancourt*
University of Puerto Rico, Mayagüez, Puerto Rico

Christopher A. Davis
National Center for Atmospheric Research†, Boulder, Colorado

1. INTRODUCTION

Despite recent efforts, predictions of tropical cyclone (TC) intensity change continue to have limited success (DeMaria et al. 2007). Particularly challenging is the prediction of rapid intensification (RI), which the National Hurricane Center (NHC) defines as an increase in the maximum sustained surface wind speed of at least 15.4 ms^{-1} in a 24-hour period (NHC 2011).

Understanding TC inner core dynamics, as well as their relationship with the environment, is believed to be necessary to predict RI occurrence (Kaplan and DeMaria 2003). Davis et al. (2008) evaluated the performance of the Advanced Hurricane Weather Research and Forecasting (AHW) model in forecasting such rapid intensity changes during the 2005 North Atlantic season. The authors found that the AHW had difficulty simulating RI, particularly when RI occurred soon after initialization.

We perform a case study of Hurricane Earl's RI using AHW model simulations described by Davis et. al. (2010). According to the NHC TC report (Cangialosi 2011), Earl was one of the five major hurricanes of the 2010 North Atlantic season that experienced RI. Data from reconnaissance flights and satellite imagery indicate that Earl's maximum sustained surface wind speed went from 38.6 ms^{-1} (August 29, 18:00 UTC) to 59.2 ms^{-1} (August 30, 18:00 UTC), increasing 20.6 ms^{-1} over the span of a day. Interestingly, the AHW produced a simulation of Hurricane Earl with almost no intensification (0.7 ms^{-1} increase in maximum wind in 24-hours) followed closely by a simulation that captured the RI event more accurately (14.0 ms^{-1} increase in maximum wind in 24-hours) (Figure 1). Throughout this study, we refer to the first forecast as the unsuccessful simulation and to the second one as the successful simulation.

The purpose of this study is to assess the environmental and structural characteristics that led to Hurricane Earl's simulated RI. Our approach is to first compare the aforementioned unsuccessful and successful AHW simulations on a large scale by examining the environmental vertical wind shear. We chose this parameter because it is often considered an unfavorable factor for TC intensification. Vertical wind shear can advect the heat and moisture necessary for convection away from the inner core of the storm (Gray 1968), or can tilt the vortex, producing an anomaly that inhibits convection (DeMaria 1996).

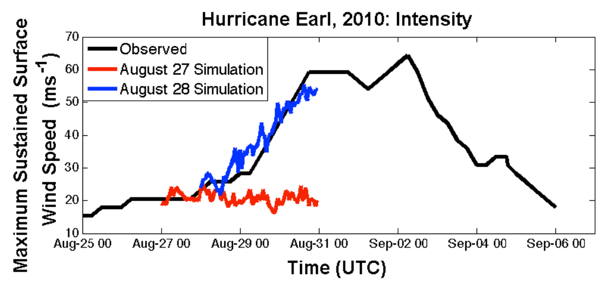

Figure 1. Evolution of Hurricane Earl's maximum wind speed. The simulation starting in August 27 was unsuccessful in predicting intensification, while the simulation starting in August 28 closely followed the observed RI.

Subsequently, we compare the simulations in terms of Hurricane Earl's vortex characteristics. We examine the local rate of change of the relative vorticity (ζ) in isobaric coordinates, which is given by:

$$\frac{\partial \zeta}{\partial t} = -\vec{V} \bullet \nabla(\zeta + f) - \omega \frac{\partial \zeta}{\partial p} - (\zeta + f)\nabla \bullet \vec{V} + \hat{k} \bullet \left(\frac{\partial \vec{V}}{\partial p} \times \nabla \omega \right) \quad (1)$$

where p is the pressure, $\vec{V}$ is the horizontal wind velocity vector, f is the absolute vorticity or Coriolis parameter, and ω is the vertical wind velocity in pressure coordinates. The area-average of the relative vorticity is defined as the circulation of the storm. Thus, we examine the vorticity equation (1) to identify the processes by which the successful simulation developed a stronger circulation.

Our expectation is that the mechanism by which the AHW rapidly intensified Earl in the successful simulation is the mechanism by which the observed Earl rapidly intensified. To verify this, our results need to be validated with observations of the storm's environmental and structural characteristics. This analysis contributes to the understanding of how rapid intensification occurs, which is beneficial for improving the accuracy of intensity forecasting.

The rest of this manuscript is organized as follows. Section 2 describes the data set and the methods applied to analyze Hurricane Earl's simulated RI, while section 3 discusses the results of this analysis. We provide some concluding remarks in section 4.

**Corresponding author address*: Diamilet Pérez-Betancourt, Dept. of Physics, P.O. Box 9000, Mayagüez, Puerto Rico, 00691, e-mail: *diamilet@gmail.com*.

†The National Center for Atmospheric Research (NCAR) is sponsored by the National Science Foundation.

2. METHODS

The simulations of Hurricane Earl analyzed in this study were produced by the AHW model, which is derived from the Advanced Research Weather Research and Forecasting (ARW) model (Davis et al. 2008). These simulations, based on ARW version 3.2, were generated as part of the National Oceanic and Atmospheric Administration's Hurricane Forecast Improvement Project (HFIP). One goal of HFIP is to improve the RI forecast skill (Davis et al. 2010). The HFIP does this by performing retrospective model runs for testing. The retrospective forecasts are simulations produced after the hurricane season with the same data available for initialization that existed in real time, but with an improved version of the model. In other words, an upgraded version of the AHW was used to reproduce forecasts for the past season. In this study, two retrospective simulations of Hurricane Earl were examined.

For these runs, the AHW was initialized via an ensemble Kalman filter data assimilation system consisting of 96 members (Torn 2010). An outer domain of coarse 36 km horizontal grid spacing was used to simulate the Atlantic basin. A double-nested domain was placed inside the parent domain to generate high-resolution forecasts. These nests had horizontal grid increments of 12 km and 4 km. They were centered on each storm as described by Davis et al. (2008). We examined the model output from the coarse domain because it provides better spatial coverage to study large-scale processes, and from the 4 km nested domain because it has the best spatial resolution to examine the storm's inner structure.

The initial time of the AHW unsuccessful simulation is August 27, 2010 at 00:00 UTC. This simulation produced only a 0.7 ms^{-1} maximum wind increase during the 24 hours when the observed RI of Earl occurred. The initial time of the successful simulation, is August 28, 00:00 UTC. This simulation was closer to the observations, producing a 14.0 ms^{-1} maximum wind increase. Although these forecasts go out to at least 5 days, we hypothesize that the differences between the simulations can be identified within the first 72-hours. Therefore, we examined the parameters near the time the forecasts were initialized.

The environmental and inner core characteristics of both successful and unsuccessful simulations of Earl were examined by computing area-averages of the quantities over four different radii (r) from the center of the storm (200, 300, 400 and 500 km). This was done to verify that the differences between the simulations were consistent at multiple scales. The storm center was obtained from the AHW track forecasts. There was no significant difference in SST along the two track forecasts during the first 72 hours; therefore it is not likely that the track difference caused the intensity difference. Rather, the tracks diverged after the difference in intensity became clear. Thus, the differences in track are not analyzed in detail in this study.

The influence of the environmental vertical wind shear was examined by calculating the area average of the wind vector difference between two pressure levels. The calculation of the standard deep-layer wind shear (850-200 hPa) was followed by the calculation of the mid-layer wind shear (850-500 hPa). The mid-layer wind shear could be more relevant at early stages of TC development where the circulation may not extend to 200 hPa.

The storm's inner structure was studied by examining the divergence (stretching) term of the vorticity equation (1), $-(\zeta + f)\nabla \bullet \vec{V}$. The divergence term can change the relative vorticity in the model runs in two different ways:

(i) At similar divergence, the simulation that starts with a stronger cyclonic circulation (higher relative vorticity) near the surface will continue to have a stronger circulation.

(ii) At similar initial vorticity, the local rate of change of the relative vorticity will depend on the divergence or convergence of air.

The divergence of a fluid can be expressed through the mass continuity equation as:

$$\nabla \bullet \vec{V} = -\frac{\partial \omega}{\partial p} \qquad (2)$$

Upward motion is associated with convergence near the surface, while downward motion is associated with divergence near the surface.

The mass flux, or area-average vertical transport of mass, indicates whether upward or downward motion is occurring in the atmosphere. Vertical profiles of the mass flux were compared between the two simulations to identify convergence or divergence of air.

The mass flux can be affected by the water vapor content in the environment of clouds. Entrainment of dry air into the inner core in the mid-troposphere can produce downdrafts and divergence of air near the surface. Thus, vertical profiles of the average relative humidity were also produced for both simulations. We examine the environmental influences of the relative humidity by using an averaging radius of 400 km and at the initial time. For an averaging radius of 200 km, the storm evolution strongly influences the humidity profile. To separate the environment from the inner structure more clearly, we eventually compute the average of humidity in rings instead of only circles.

The influence of the advection terms of the vorticity equation described by the first and second terms in (1) was left for future investigation. The horizontal advection of absolute vorticity may be related to the environmental vertical wind shear. Finally, the influence of the tilting term (fourth term in equation (1)) was not considered because it is typically less important on horizontal scales of 100 km or more.

3. RESULTS AND DISCUSSION

3.1 *Environmental characteristics*

Time series of the average deep-layer vertical wind shear are shown in Figure 2a. For all four averaging radii, and for both simulations, the initial vertical wind shear was low (1-3 ms^{-1}) compared to what is commonly considered unfavorable for TC intensification (about 10 ms^{-1}). While the unsuccessful simulation experienced stronger deep-layer wind shear, it did not do so until after the intensities in the two simulations started diverging from each other. These results suggest that the wind shear did not significantly influence the intensification of the successful simulation. Time series of the average shallow-layer vertical wind shear (Figure 2b) confirm this result. For all four averaging radii, the shallow-layer wind shear was similar for both simulations at the beginning.

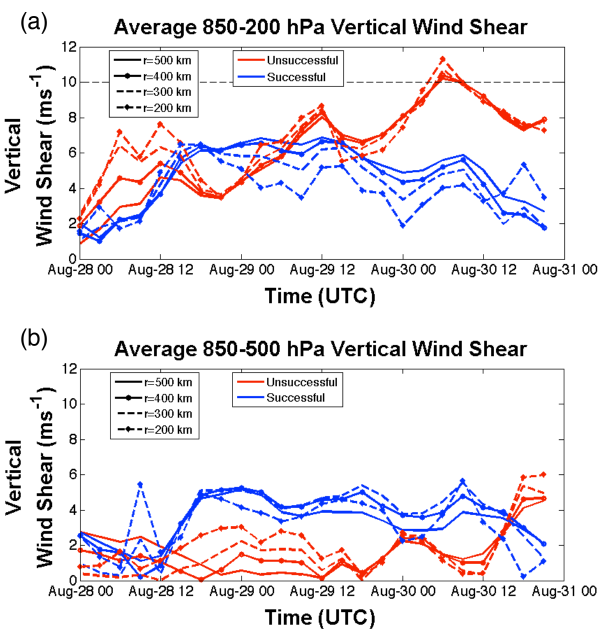

Figure 2. Average (a) 850-200 hPa vertical wind shear and (b) 850-500 hPa vertical wind shear for the unsuccessful simulation (red lines) and the successful simulation (blue lines).

3.2 *Inner structure characteristics*

Vertical profiles of the circulation for both simulations are shown in Figure 3. The successful simulation initially had a stronger circulation than the unsuccessful simulation throughout the troposphere. By examining the stretching term of the vorticity equation (1), we could anticipate that the successful simulation would develop an even stronger circulation, assuming a comparable divergence profile, since the initial circulation was stronger.

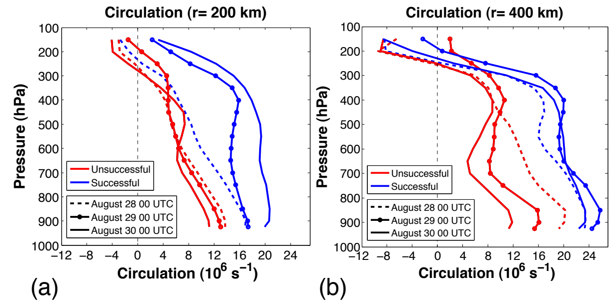

Figure 3. Circulation (area-average of the relative vorticity) for the unsuccessful simulation (red lines) and the successful simulation (blue lines) with averaging radius of (a) 200 km and (b) 400 km.

Vertical profiles of the relative humidity are shown in Figure 4. The unsuccessful simulation started with a drier profile throughout the troposphere, especially within the storm circulation. Dry air in the mid-troposphere makes the atmosphere susceptible to downdrafts. These may lead to downdrafts that produce divergence in the lower troposphere, a negative factor for increasing cyclone intensity. It is also possible that the dry air directly limits the development of deep convection. Note that the data assimilation system integrates without the 4-km nest. When the nest is switched on at the start of the forecast, the atmosphere must first saturate before precipitation begins because there is no cumulus parameterization on this domain.

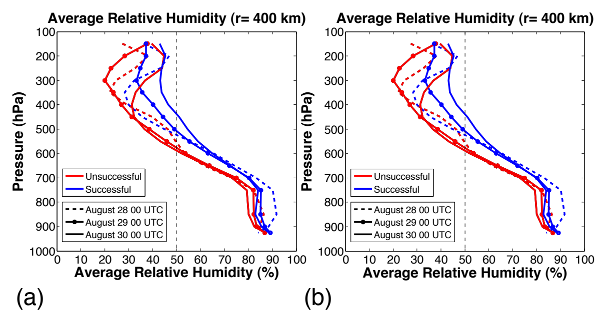

Figure 4. Average relative humidity for the unsuccessful simulation (red lines) and the successful simulation (blue lines) with averaging radius of (a) 200 km and (b) 400 km.

The vertical profiles of the mass flux, which were computed to examine the divergence in the stretching term of the vorticity equation (1), are shown in Figure 5. The mass flux increased rapidly in the mid-troposphere (strong mid-tropospheric convergence developed) within the first 24 hours in the successful forecast. This occurred before any significant change in the circulation occurred near the surface (Figure 3). We hypothesize that the rapid increase in the mass flux at the mid-troposphere is related to the initial higher moisture content in the successful simulation.

At the same time, a rapid increase in the relative humidity at mid-levels was related to this rapid increase in mass flux in the successful simulation. Convergence of air at the surface is necessary for convection to occur.

The convection itself moistens the air at mid-upper levels. Although the unsuccessful simulation experienced some moistening, the air was still dry compared to the successful simulation.

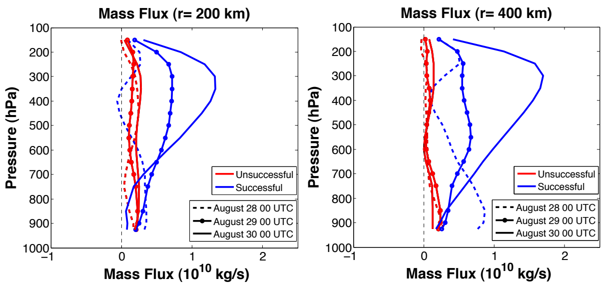

(a) (b)

Figure 5. Mass flux (area-average of the mass vertical transport) for the unsuccessful simulation (red lines) and the successful simulation (blue lines) with averaging radius of (a) 200 km and (b) 400 km.

A rapid increase of the circulation at the mid-troposphere also occurred during the first 24 hours in the successful forecast. After this deep vortex had been established, mass flux (and lower tropospheric convergence) continued to increase. After 48 hours, the successful simulation developed a mass flux profile typical of a mature hurricane, with convergence in the lower and middle troposphere (positive slope) and divergence aloft (negative slope). This lead to Hurricane Earl's RI.

4. CONCLUSIONS

The purpose of this study has been to identify the environmental and storm structure characteristics that led to Hurricane Earl's simulated RI in the AHW model. The AHW model produced this successful simulation following a simulation that was unsuccessful in predicting Earl's RI. We compared the two simulations by studying the environmental vertical wind shear and the vorticity equation.

On the large scale, our results suggest that the environmental vertical wind shear did not significantly influence the RI of the successful simulation. On the storm scale, we found that the relative humidity and circulation were initially higher for the successful simulation than for the unsuccessful simulation. We concluded that the high moisture content in the mid-troposphere in the successful simulation eased the rapid increase of the mass flux at this level. As a result, the humidity and circulation also increased rapidly at the mid-troposphere. RI at the lower troposphere followed.

Although there is still much to examine, these results provide a basis for further research to better understand the development of RI. Future work includes averaging the environmental parameters in rings to separate them from the inner structure, and examining other structural aspects of the storm's thermodynamics. In addition, it is important to verify the results with other AHW simulations of Earl and compare the results to available observations to determine if the successful simulation was successful for the right reasons. Finally, the results should be verified by examining other storms that experienced RI.

ACKNOWLEDGEMENTS

This work was performed under the auspices of the Significant Opportunities in Atmospheric Research and Science Program (SOARS). The first author would like to thank Christopher Davis for his extensive collaboration with this project. Kimberly Kosmenko's comments on the manuscript throughout its evolution are also much appreciated. Special thanks are extended to SOARS staff Rajul Pandya, Rebecca Haacker-Santos, and Moira Kennedy, and to the Mesoscale and Microscale Meteorology Division at NCAR. Ryan Torn (University at Albany-State University of New York) produced the model output utilized in this project. Sherrie Fredrick and David Ahijevych kindly provided help with the NCAR Command Language scripts. Finally, the 2011 SOARS protégés and Andrea Feldman's suggestions were very helpful in improving the manuscript.

5. REFERENCES

Cangialosi, J. P., 2011: Tropical cyclone report, Hurricane Earl, 25 August- 4 September 2010. NOAA/National Hurricane Center, 29 pp.

Davis, C., W. Wang, S. S. Chen, Y. Chen, K. Corbosiero, M. DeMaria, J. Dudhia, G. Holland, J. Klemp, J. Michalakes, H. Reeves, R. Rotunno, and Q. Xiao, 2008: Prediction of landfalling hurricanes with the Advanced Hurricane WRF Model. *Mon. Wea. Rev.*, **136**, 1990-2005.

______ , ______ , and J. Dudhia, 2010: Does increased horizontal resolution improve hurricane wind forecasts?. *Wea. Forecasting*, **25**, 1826-1841.

DeMaria, M., 1996: The effect of vertical shear on tropical cyclone intensity change. *J. Atmos. Sci.*, **53**, 2076-2087.

______ , J.A. Knaff, and C. Sampson, 2007: Evaluation of long-term trends in tropical cyclone intensity forecasts. *Meteor. Atmos. Phys.*, **97**, 19-28.

Gray, W. M., 1968: Global view of the origin of tropical disturbances and storms. *Mon. Wea. Rev.*, **96**, 669-700

Kaplan, J., and M. DeMaria, 2003: Large-scale characteristics of rapidly intensifying tropical cyclones in the North Atlantic basin, *Wea. Forecasting*, **18**, 1093-1108.

National Hurricane Center, cited 2012: Glossary of NHC terms. [Available online at http://www.nhc.noaa.gov/aboutgloss.shtml.]

Torn, R. D., 2010: Performance of a mesoscale ensemble Kalman filter (EnKF) during the NOAA High-Resolution Hurricane Test. *Mon. Wea. Rev.*, **138**, 4375-4392.